IN-39
64798
P. 26

# Development of Advanced Structural Analysis Methodologies for Predicting Widespread Fatigue Damage in Aircraft Structures

C. E. Harris, J. H. Starnes, Jr. and J. C. Newman, Jr.
*Langley Research Center, Hampton, Virginia*

August 1995

# Development of Advanced Structural Analysis Methodologies for Predicting Widespread Fatigue Damage in Aircraft Structures

by

Charles E. Harris,
James H. Starnes, Jr.
James C. Newman, Jr.

Research and Technology Group
NASA Langley Research Center
Hampton, VA 23681

## Abstract

NASA is developing a "tool box" that includes a number of advanced structural analysis computer codes which, taken together, represent the comprehensive fracture mechanics capability required to predict the onset of widespread fatigue damage. These structural analysis tools have complementary and specialized capabilities ranging from a finite-element-based stress-analysis code for two- and three-dimensional built-up structures with cracks to a fatigue and fracture analysis code that uses stress-intensity factors and material-property data found in "look-up" tables or from equations. NASA is conducting critical experiments necessary to verify the predictive capabilities of the codes, and these tests represent a first step in the technology-validation and industry-acceptance processes. NASA has established cooperative programs with aircraft manufacturers to facilitate the comprehensive transfer of this technology by making these advanced structural analysis codes available to industry.

# Nomenclature

$a$     = crack half length
$a_i$    = initial crack half length
$B$     = plate thickness
CTOA = crack tip opening angle
CTOD = crack tip opening displacement
$d_r$     = spacing of MSD cracks
$L_i$     = total initial crack length for MSD
$L_r$     = length of small MSD cracks
MSD  = multiple site damage (cracks)
$M$     = bending moment
$N_i$     = stress resultants as designated by the subscript
$p$     = internal pressure
$P_i$     = frame and stringer loads as designated by the subscript
$S$     = applied far-field stress
$S_n$    = net-section stress
$T$     = torsional load
$V$     = vertical shear load
$W$     = plate width
$\sigma_{ys}$   = yield stress
$\sigma_u$    = ultimate tensile strength

# Introduction

The National Aeronautics and Space Administration (NASA) Airframe Structural Integrity Program (NASIP) was initiated in 1990 after extensive consultations with the U.S. airframe manufacturers, airline operators, and the Federal Aviation Administration (FAA). The objective of the program is to develop advanced technology that can be used by the U.S. industry to maintain economically the aging commercial transport fleet while insuring continuous airworthiness. The program is a formal cooperative program with the U.S. aircraft industry and is part of the U.S. Government Strategic Plan for Aging Aircraft Research that includes FAA and NASA activities. While the development of cost-effective nondestructive-inspection technology is a major part of the NASA Airframe Structural Integrity Program, the present paper only addresses the development of a structural integrity analysis methodology for predicting the onset of widespread fatigue damage.

The ability to predict analytically the onset of widespread fatigue damage in fuselage structures requires methodologies that predict fatigue crack initiation, crack growth, and residual strength. Mechanics-based analysis methodologies are highly desirable because differences in aircraft service histories can be addressed explicitly and rigorously by analyzing different types of aircraft and specific aircraft within a given type. Each aircraft manufacturer has developed mature in-house durability and damage-tolerance design and analysis methodologies that are based on their product development history. To enhance these existing successful methodologies, NASA has adopted the concept of developing an analytical "tool box" that includes a number of advanced structural analysis computer codes which, taken together, represent the comprehensive fracture mechanics capability required to predict the onset of widespread fatigue damage. The structural analysis tools have complementary and specialized capabilities ranging from a nonlinear finite-element-based stress-analysis code for two- and three-dimensional built-up structures with cracks to a fatigue and fracture analysis code that uses stress-intensity factors and material-property data found in "look-up" tables or from equations. The development of these advanced structural analysis methodologies has been guided by the physical evidence of the fatigue process assembled from detailed tear-down examinations of actual aircraft structure. In addition, NASA is conducting critical experiments necessary to verify the predictive capability of these codes and to provide the basis for any further methodology refinements that may be required. The NASA experiments are essential for analytical methods development and verification, but represent only a first step in the technology-validation and industry-acceptance processes. Each industry user of this advanced methodology must conduct an assessment of the technology, conduct an independent verification, and determine the appropriate integration of the new structural analysis methodologies into their existing in-house practices. NASA has established cooperative programs with U.S. aircraft manufacturers to facilitate this comprehensive transfer of this technology by making these advanced methodologies available to industry.

A detailed description of the methodologies under development is presented in the present paper. A brief description of the structural analysis computer codes in the NASA tool box is given in the paper. Beta-site testing of the various structural analysis codes is currently underway and the technology that is being transferred to industry is highlighted. The status of the analytical residual-strength prediction methodology is discussed in the context of an application to a generic stiffened aluminum thin-shell

3

structure fabricated by a riveted-skin construction method. The status of the experimental verification of the methodology is also discussed.

## Structural Analysis Computer Codes for Structural Integrity

The NASA tool box outlined in Table 1 contains several structural analysis computer codes that have been developed to meet specific specialized engineering requirements. Even though the data in Table 1 suggest that the codes may have overlapping capabilities, each code has unique capabilities that are required to address specific durability and damage-tolerance issues for a wide variety of engineering applications. The determination of the number of aircraft service hours that is related to the onset of widespread fatigue damage includes analyses for crack initiation, fatigue crack growth, and residual strength. Therefore, the computational capability required to predict analytically the onset of widespread fatigue damage must be able to represent a wide range of crack sizes from the material (microscale) level to the global structural-scale level. NASA studies indicate that the fatigue crack behavior in aircraft structure can be represented conveniently by the following three analysis scales: small three-dimensional cracks at the microscale level; through-the-thickness two-dimensional cracks at the local structural level; and long cracks at the global structural level. The computational requirements for each of these three analysis scales are described in the following paragraphs.

The first analysis scale and corresponding computational capability represents the fracture mechanics of small cracks that exhibit three-dimensional crack-growth behavior. The existence and growth of these small cracks do not affect the global structural deformation states or internal load distributions. Examples of these cracks are surface and corner cracks that initiate at the edges of plates or at holes. Stress-intensity-factor solutions are typically obtained from computational procedures such as the finite element analysis method. The ZIP3D computer code [1] has been developed to model three-dimensional crack configurations and to calculate the corresponding stress-intensity factors. This finite element analysis code uses an eight-node element and can be used to analyze stationary and growing cracks under cyclic elastic-plastic conditions, including the effects of crack closure. The FRANC3D code [2] also has solid modeling capabilities for three-dimensional geometries based on the boundary element method. For those crack configurations and general loading conditions that may occur for various structural components, weighting-function solutions are being developed

from the numerical results of parametric studies. These weighting-function equations are particularly useful because the stress-intensity-factor solutions can be obtained from a stress analysis of the uncracked structure. Stress-intensity-factor solutions are currently being generated for cracks that initiate at countersunk rivet holes. Loading conditions include interference-fit stresses, clamp-up stresses, and loads transferred through a rivet. These stress-intensity-factor solutions may then be used as input data for the FASTRAN II code [3] to predict fatigue-crack growth. The FASTRAN II code is based on the mechanics of plasticity-induced crack closure. The effects of prior loading history on fatigue behavior, such as crack-growth retardation and acceleration, are computed on a cycle-by-cycle basis. The code will predict the growth of cracks exhibiting the "small-crack effect" as well as two- and three-dimensional cracks exhibiting the classical Paris-law crack-growth behavior. The code has been shown to be especially effective for predicting fatigue-crack-growth behavior in structures subjected to aircraft spectrum loads. The ZIP3D, FRANC3D, and FASTRAN II codes operate efficiently on engineering workstations, and FASTRAN II also operates on personal computers.

The second analysis scale and corresponding computational capability represent the fracture mechanics of fatigue cracks that extend through the thickness of a skin or stiffener and are no longer three-dimensional in their crack-growth behavior. Two-dimensional analyses are typically quite adequate for predicting crack growth. However, accurate modeling of structural details is required to provide high-fidelity results for the local stresses in a structure so that the fracture-mechanics calculations will be accurate. The FRANC2D finite element analysis code [4] has been developed for the analysis of two-dimensional planar structures and the STAGS (STructural Analysis of General Shells) nonlinear shell analysis code [5] has been developed for general shell structures. The FRANC2D code, developed by Cornell University, is a user-friendly engineering analysis code with pre- and post-processing capabilities especially developed for fracture-mechanics problems. The code operates on UNIX-based engineering workstations with X-Windows graphics and is interactive and menu driven. A unique capability of the code is the ability to predict non-self-similar crack-growth behavior. An automatic adaptive remeshing capability allows an engineer to obtain a history of the stress-intensity factors for any number of cracks in the structure and for any arbitrary crack-growth trajectory. The STAGS finite element code [5], developed by Lockheed Palo Alto Research Laboratory, provides the capability to model any general shell structure and has both geometric and material nonlinear

analysis capabilities. STAGS is particularly well suited for analyzing shells that have structural features such as frames, stiffeners, and cutouts. The code uses the Riks arc-length projection method and computes large displacements and rotations at the element level. The code has been developed especially for nonlinear stability and strength analyses. Both FRANC2D and STAGS can calculate the history of the stress-intensity factors for a growing crack that are compatible with FASTRAN II so that fatigue crack-growth analyses may be performed. Other crack-growth models may also be used. STAGS and FRANC2D operate on engineering workstations and mainframe computers.

The third analysis scale and corresponding computational capability represent structures with long cracks that change the internal structural load distribution, that exhibit behavior strongly affected by structural details, and that affect the residual strength of the structure. In addition, the fracture mechanics of ductile materials such as 2024-T3 aluminum alloy often requires an elastic-plastic stress-analysis capability that predicts stable tearing and fracture. Furthermore, nonlinear geometric effects, such as crack bulging in shell structures, also significantly affect residual-strength predictions. All of these complexities are present in a fuselage shell structure and must be represented in a residual-strength analysis of the fuselage. NASA has developed a unique capability that integrates the fracture topology modeling capabilities of FRANC3D with the general shell analysis capabilities of STAGS into an integrated FRANC3D/STAGS analysis procedure [6]. The automatic adaptive remeshing capability of FRANC3D and the geometric nonlinear stress-analysis capability of STAGS provides the analysis basis required to predict the crack-growth, crack-turning and crack-arrest behavior exhibited by pressurized shell structures in damage-tolerance tests. Such a residual-strength analysis capability for a fuselage shell structure requires a suitable fracture criterion. Current plans include implementing the critical crack-tip opening-angle criterion (CTOA), the T* criterion, and the K-R curve criterion into the STAGS analysis code for predicting the residual strength of shell structures. This capability is described in greater detail in the following sections of this paper. For simple two-dimensional plane-stress or plane-strain fracture mechanics problems, the ZIP2D special-purpose finite element code [7] has proven to be very accurate and computationally efficient. The integrated FRANC3D/STAGS analysis procedure currently operates on high-level workstations or on mainframe computers, and ZIP2D operates on workstations.

Several of the advanced durability and damage-tolerance analysis capabilities developed in the NASA program will also be implemented in the NASGRO analysis code [8]. NASGRO is a general-purpose damage-tolerance analysis code being developed by NASA Johnson Space Center. The code is based on fracture mechanics principles and may be used to compute stress-intensity factors, fatigue crack growth, critical crack sizes, and the limit of safe life. An extensive library of stress-intensity factors may be used with NASGRO or solutions may be obtained from a boundary element analysis capability using the FADD analysis code [9]. NASGRO also has an extensive material property library which includes most aluminum alloys, titanium alloys, and steels commonly used in the aerospace industry. Fatigue crack growth may be computed from a crack-closure mechanics model or from one of several empirical models commonly used by industry. NASGRO is used extensively throughout the aerospace industry. FADD was developed at the University of Texas and uses the distributed-dislocation method to compute stress-intensity factors. This approach combines a highly accurate stress-intensity factor analysis with the modeling simplicity of the boundary element analysis method. FADD is also available in a stand-alone version and is currently being tested by industry at beta-site locations. NASGRO operates on engineering workstations and personal computers. FADD is also available as a stand-alone code and operates on personal computers.

## Residual-Strength Analysis Methodology

The structural analysis computer codes under development in the NASA Airframe Structural Integrity Program are being integrated into an analytical methodology for predicting the residual strength of a fuselage structure with one or more cracks. The analytical prediction of the residual strength of a complex built-up shell structure, such as a fuselage, requires the integration of a ductile fracture criterion, a fracture-mechanics analysis, and a detailed stress analysis of the structure. The crack-tip opening-angle (CTOA) criterion has been experimentally verified to be a valid fracture criterion for mode I stress states in thin and moderately thick (0.5-inch-thick or less) aluminum alloys. The CTOA criterion has been demonstrated to be valid for predicting the link-up of a long lead crack with small fatigue cracks ahead of the advancing lead crack. This fracture criterion has been implemented into the STAGS geometric and material nonlinear finite-element-based shell analysis code to provide an integrated structural-integrity analysis methodology. The capability to model a growing crack that may extend in a non-self-similar direction has been added to the STAGS

code along with an automated mesh refinement and adaptive remeshing procedure. The topological description of the growing crack is provided by the FRANC3D fracture mechanics code. The geometric nonlinear behavior of a stiffened fuselage shell is currently under study for internal pressure loads combined with fuselage body loads that produce tension, compression and shear loads in the shell. A detailed description of this capability is described in the following paragraphs.

## *The CTOA Fracture Criterion*

The critical crack-tip opening-angle (CTOA), or equivalently, the crack-tip opening-displacement (CTOD), fracture criterion is a "local" approach to characterizing fracture. In contrast, the J-integral or J-R curve criterion is based on global deformations and has been found to be specimen and crack-size dependent for structures with large amounts of stable tearing. The constant CTOA (or CTOD) criterion has been used to predict the variations in J-R curves due to differences in crack sizes and specimen types. Therefore, a local crack-tip displacement is a more fundamental fracture parameter than the J-integral representation for local strain-controlled fracture processes such as stable tearing and void coalescence.

Stable crack growth in metallic materials has been studied extensively using elastic-plastic finite element methods [10-17]. These studies were conducted to examine various local and global fracture criteria such as the CTOA or CTOD criteria, the crack-tip stress or strain criteria, the strain-energy release-rate criterion, the J-integral criterion and the tearing modulus criterion. It was shown by de Koning [12] that the CTOA is nearly constant from crack-growth initiation to failure in an aluminum alloy. Shih, et al. [15] and Kanninen, et al. [16] showed that the CTOA at crack-growth initiation is apparently larger than the value needed for stable crack growth in fracture analyses of both steel and aluminum alloys. Brocks and Yuan [18], and Demofunti and Rizzi [19] found that CTOA is nearly constant for various materials and thicknesses after a small amount of crack growth. Newman [17] used the critical CTOD values obtained from compact tension specimens to predict failure loads to within 10 percent of the test results for several other crack configurations for two aluminum alloys and a ductile steel. Paleebut [20] also measured the CTOD at the initiation of stable tearing in aluminum alloys and these measured values of CTOD agree well with Newman's numerical results [17]. The results of tests conducted by Hellman and Schwalbe [21] show good correlation between the CTOD values measured at the initial fatigue-crack-tip location

for stable tearing in a variety of specimen types. More recently, Newman, Dawicke, Sutton and Bigelow [22] used a high-resolution microscope with a video recording system to measure the CTOA during stable crack growth in 2024-T3 aluminum. These test results show that the CTOA is constant for both center-cracked panels and compact tension specimens over a wide range of crack- extension lengths after a small (approximately one sheet thickness) amount of crack growth.

Simple plastic-zone models that are based on linear-elastic stress-intensity factors can be adjusted to fit experimental data and then used to predict crack link-up for relatively simple structural geometries. While these methods predict the correct trends in crack link-up behavior, they may be difficult to apply to analyses of complex structural details that are characteristic of a fuselage structure. The CTOA criterion can be effectively implemented into a finite element analysis code provided that the code has elastic-plastic deformation and crack-growth simulation capabilities. These capabilities exist in the STAGS geometric and material nonlinear shell analysis code, but analyses of large-scale problems must currently be conducted on a high-performance mainframe computer. After thorough experimental verification of the residual-strength analysis methodology, it is anticipated that the methodology can be simplified by taking advantage of appropriate engineering approximations.

## Verification of the CTOA Fracture Criterion Using Flat-Panel Test Data

An extensive test program has been conducted to interrogate experimentally the characteristics of the CTOA criterion and to establish its validity as a fracture criterion for thin-sheet 2024-T3 aluminum. A schematic of the four basic flat-panel geometries used to verify the elastic-plastic finite-element code and the CTOA criterion for mode I fracture is shown in Figure 1. The blunt- notch panel was used to verify the finite element analysis code used to compute plastic deformation fields and large displacements. Measurements of far-field displacements and the local displacements inside the open holes at the ends of the crack were accurately predicted by the finite element analysis for large-scale plastic deformations.

The center-crack and three-hole-crack panels were used to measure the load (or far-field applied stress) as a function of crack extension and the CTOA during stable tearing. Because the tests were conducted at a specified controlled displacement rate, crack extension was measured well beyond the maximum load observed during the

test. Stable tearing was quite extensive in the three-hole-crack specimen because the crack driving force is reduced as the crack approaches the two large open holes in a manner that is similar to the behavior of cracks in stiffened panels. A high-resolution long-focal-length microscope was used to record the stable-tearing results. The microscope image was videotaped, digitized, and recorded in a computer file. The tearing event was then analyzed on a frame-by-frame basis and the critical opening angle was measured throughout the fracture event. A typical CTOA measurement is shown in Figure 2. As can be seen in the figure, the opening angle is relatively insensitive to the length over which the angle is measured. The results of a three-hole-crack panel test are given in Figure 3. After an initial transition region, the CTOA is constant throughout the stable-tearing process. The initial transition region is caused by a three-dimensional effect that occurs as the crack tunnels and transitions from flat- to slant-crack growth. Over 63 mm (2.5 in.) of stable tearing was recorded and the CTOA values were nearly constant. Measurements such as these were also made for center-crack and three-hole-crack panels of various widths, crack lengths, and sheet thicknesses ranging from 1.02 mm (0.040 in.) to 2.29 mm (0.090 in.). Also, measurements of the CTOA were obtained for compact tension specimens. In all cases, the measured CTOA was approximately 6.0° for cracks oriented in the LT direction of the sheet and 5.1° for cracks oriented in the TL direction, where L designates the principal rolling direction of the sheet and T designates the direction transverse to the principal rolling direction. A complete description of these test results is given in reference 22.

An elastic-plastic finite element analysis was conducted for every test-panel configuration reported in reference 22. A typical stress-analysis result for a center-crack panel is shown in Figure 4. The analysis assumes plane-stress conditions and the applied stress as a function of crack extension is predicted using a CTOA value of 6.0°. Test results for three sheet thicknesses are shown in the figure. As can be seen in the figure, there is virtually no thickness effect on the test results for this range of sheet thicknesses. The finite element analysis accurately predicted the maximum applied stress and the crack extension before and after the maximum value of the test load had been applied. A complete description of the finite element analysis code and the analysis method along with more results can be found in reference 22.

To verify further the CTOA fracture criterion, a series of panels with multiple-site cracks (MSD) was also tested to determine the conditions leading to crack link-up.

Under sponsorship by the FAA, the Foster-Miller Company [23] conducted a number of fracture tests on 508 mm (20.0 in.) wide panels with one-, three-, five-, and seven-crack configurations. Each crack configuration has a long center crack with small MSD cracks symmetrically located ahead of the long center crack. NASA conducted a finite element analysis of each panel. The analytical and experimental results for a panel with a 305 mm. (12.0 in.) long center crack and two 12.60 mm (0.50 in.) long cracks on both sides of the center crack with a 25.4 mm (1.0 in.) long ligament between the small cracks are given in Figure 5. By using a CTOA value of 5.1°, the finite element analysis accurately predicted the applied stress $S_1$ for the first crack link-up, the maximum stress $S_2$ sustained by the panel, and the applied stress $S_3$ for the second crack link-up. Catastrophic failure of the panel occurred after the second crack link-up. Descriptions of the complete Foster-Miller test results and analyses using other fracture criteria are given in reference 23 and the results of additional analyses using the CTOA criterion are given in reference 22.

A summary comparing several test results and the finite element analysis predictions for the panels with multi-site damage or MSD is given in Figure 6. For convenience, the applied far-field stress $S$ has been divided by the yield stress $\sigma_{ys}$ of 2024-T3 aluminum alloy. Also shown for comparison is the applied stress at which the ligament between the cracks or the edge of the specimen was fully yielded. The long center cracks for the four examples shown in the figure are of different lengths. The CTOA fracture criterion and the elastic-plastic finite element analysis accurately predicted the failure stresses for all flat-panel test results. Also, the results in the figure indicate that the ligament between the cracks for the MSD crack configurations is fully yielded at a stress level well below the applied stress level at crack link-up. This comparison suggests that a simple fracture criterion such as the "ligament net-section stress equal to yield stress" criterion should be used with some degree of caution. The effects of MSD on the residual strength of a 1.016 m (40.0 in.) wide flat panel with a 0.356 m (14.0 in.) long center crack is illustrated by the analytical results shown in Figure 7. The crack lengths and spacings are plotted along the abscissa of the figure and the applied far-field stress is plotted along the ordinate. The dashed lines represent the crack-extension behavior of the panel with only a single long lead crack of the indicated lengths. The solid line shows the crack-extension behavior due to the MSD cracks ahead of the long lead cracks. There is a reduction in the residual strength of the panel due the presence of MSD. In this example, both the long lead crack and the first small crack grew toward each other prior to crack link-up.

11

The experimental and analytical results presented herein verify the CTOA fracture criterion for predicting the residual strength of flat panels with cracks undergoing mode I fracture behavior. Further testing is required to verify the criterion for predicting the residual strength of complex stiffened shell structures. The CTOA criterion must be extended to mixed-mode loading conditions. Also, numerical procedures for crack extension under mixed-mode loading conditions must be implemented into an elastic-plastic shell analysis code. And finally, the ability to predict crack trajectories accurately and to model curved crack growth must be developed. The next section describes the stiffened shell structural analysis methodology being developed for analyzing a fuselage structure and to predict its residual strength accurately.

### *Development of a Geometric Nonlinear Finite Element Shell Analysis Code*

The STAGS nonlinear finite element analysis code is being modified to include the capability of conducting crack-growth and residual-strength analyses for stiffened fuselage shell structures subjected to combined internal pressure and mechanical loads. STAGS was originally developed to predict the strength, stability and nonlinear response of non-axisymmetric or general shells and includes analyses for both geometric and material nonlinear behavior. The nonlinear solution algorithm used in STAGS is based on Newton's method and includes both the modified and full versions of Newton's method. Large rotations are represented by a co-rotational algorithm at the element level and the Riks arc-length projection method is used to integrate past limit points. The finite element library includes nonlinear beam, plate, and shell elements. Complex stiffened shell structures can be modeled to include as many finite elements as required to represent accurately the response of each structural member in the stiffened shell of interest. The computational efficiency of the code allows nonlinear analyses of models with over 100,000 degrees of freedom to be conducted in a reasonable amount of computer time. Both self-similar and non-self-similar crack-growth prediction capabilities have been added to STAGS for predicting crack growth in a shell that is in a nonlinear equilibrium state. The crack-growth analysis used in FRANC3D/STAGS is based on a virtual crack extension analysis that calculates the strain energy release rate for nonlinear shells with mixed-mode crack growth including shell wall bending. A load relaxation capability is used to represent the local load redistribution that occurs as a crack grows in the shell and Newton's method is used to

maintain nonlinear equilibrium as the crack propagates. Nonlinear adaptive mesh refinement is used to determine the necessary finite element model changes as the crack propagates.

The general strategy for developing the nonlinear structural analysis methodology for predicting residual strength of stiffened shells with cracks is shown in Figure 8. Large-scale global models of a stiffened fuselage shell of interest are developed and nonlinear analyses are conducted to determine the internal load distribution and general response of the shell as shown in the upper left of the figure. A hierarchical modeling approach is used to provide more highly refined local models which are developed based on the global model results. The local models provide the higher-fidelity solutions that are necessary to predict stress and displacement gradients near the crack discontinuity in the shell as shown in the upper right of the figure. Several local models are generated as required and analyzed to provide the detailed stress and deflection results necessary to predict crack growth and residual strength for any structural detail feature such as the longitudinal lap splice shown in the lower right of the figure. Selected curved stiffened panels and stiffened shells will be tested to provide experimental verification of the STAGS nonlinear shell analysis capability.

## Nonlinear Behavior of Stiffened Shells With Damage

An example of the hierarchical modeling strategy for nonlinear stiffened shell analysis is shown in Figure 9. The nonlinear hoop stress and radial deflection results for the global shell model of a frame and stringer stiffened aluminum shell are shown on the left of the figure. The shell has a longitudinal crack at the top of the fuselage and is loaded by 55.2 KPa (8 psi) of internal pressure. The longitudinal crack in the skin is next to a stiffener and the frame at the crack location is also broken. A curved stiffened panel model was developed with five frames and five stringers to generate the 36-skin-bay local model as shown in the upper right of the figure. This model provides more detailed stress- and deflection-gradient results near the cracked region as shown in the figure. The results shown are for a 0.508 m (20.0 in.) long skin crack with the center of the crack at the broken frame. The frames are located at the dark circumferential regions in the figure. The boundary conditions for this local model are based on the results of the global model analysis and both equilibrium and compatibility with the nonlinear global shell solution are maintained at the panel boundaries. A more refined stiffened panel model was developed with two frames and three stringers to generate

the six-skin-bay local model shown in the lower right of the figure. The hoop stress and radial deflection results shown are for a 1.016 m (40.0 in.) long crack that has grown to the frames on either side of the broken frame. The boundary conditions for this more refined local model are based on the results of the 36-skin-bay stiffened panel model and both equilibrium and compatibility with the nonlinear 36-skin-bay panel solution are maintained at the six-skin-bay panel boundaries. This hierarchical modeling and analysis approach provides the high-fidelity nonlinear stress- and deflection-gradient results needed to represent the shell behavior near the crack to the level of accuracy required to predict crack growth and residual strength accurately.

This hierarchical modeling approach has been used to determine the effects of combined internal pressure and mechanical loads on the response of a stiffened shell with a skin crack at the top of the shell. The crack is 0.254 m (10.0 in.) long initially and is located midway between the two stringers at the top of the shell and midway between two frames. The shell is subjected to the following three loading conditions: internal pressure only, internal pressure plus a down-bending moment, and internal pressure plus an up-bending moment. The axial stress resultants from the nonlinear analyses for these three loading conditions are shown in Figure 10. The axial stress resultants for the global model with internal pressure only are shown in the upper part of the figure and these results indicate that the value of the axial stress resultant is approximately 17.5 KN/m (100 lb/in.) except in the immediate vicinity of the crack where the value of the axial stress resultant is approximately 52.5 KN/m (300 lb/in.). The axial stress resultants for the global model with the internal-pressure and down-bending loads are shown in the lower left of the figure and these results indicate that the values of the axial stress resultants are approximately 52.5 KN/m (300 lb/in.) in tension at the top of the shell and approximately 52.5 KN/m (300 lb/in.) in compression at the bottom of the shell. The axial stress resultants for the global model with the internal-pressure and up-bending loads are shown in the lower right of the figure and these results indicate that the values of the axial stress resultants are approximately 52.5 KN/m (300 lb/in.) in compression at the top of the shell except in the immediate vicinity of the crack and approximately 52.5 KN/M (300 lb/in.) in tension at the bottom of the shell. The results for the local six-bay panel analyses for these three loading conditions are shown in Figure 11 for 0.254-, 0.381-, 0.508-m- (10-, 15- and 20-in.-) long cracks. The results for the internal-pressure-only load case is shown at the top of the figure and indicate that the axial stress resultant values are approximately 14.0 KN/m (80 lb/in.) in compression at the frames and are approximately 70.0 KN/m (400 lb/in.) in tension along the crack

14

boundary. The extent of these high values of axial stress resultants grows locally as the crack grows in length. The results for the internal-pressure plus down-bending load case is shown in the middle of the figure and indicate that the axial stress resultant values are approximately 31.5 KN/m (180 lb/in.) in tension at the frames and are approximately 70.0 KN/m (400 lb/in.) in tension along the crack boundary. The results for the internal-pressure plus up-bending load case are shown at the bottom of the figure and indicate that the axial stress resultant values are approximately 61.3 KN/m (350 lb/in.) in compression at the frames and are approximately 70.0 KN/m (400 lb/in.) in tension along the crack boundary. These results indicate that the complex local nonlinear behavior of the shell causes very different results for the three loading conditions. The effects of these differences on the mode I strain-energy release rate for the shell are shown in Figure 12 for the three loading conditions. The strain-energy release-rate results for increasing crack lengths are represented by the filled circles for the internal-pressure-only load case, by the filled triangles for the internal-pressure plus down-bending load case, and by the filled squares for the internal-pressure plus up-bending load case. These results indicate that the axial tension stress resultant at the crack associated with the down-bending load case decreases the strain-energy release rate by approximately 11 percent compared to the internal-pressure-only load case. The results also indicate that the axial compression stress resultant at the crack associated with the up-bending load case increases the strain-energy release rate by approximately 14 percent compared to the internal-pressure-only load case. These results suggest that the nonlinear coupling between the radial deflections and the in-plane stress resultants near the crack have a significant effect on the crack-growth and residual-strength characteristics of stiffened shell structures with longitudinal cracks.

## Summary

NASA is developing a "tool box" that includes a number of advanced structural analysis computer codes which, taken together, represent the comprehensive fracture mechanics capability required to predict the onset of widespread fatigue damage. These structural analysis tools have complementary and specialized capabilities ranging from a finite-element-based stress-analysis code for two- and three-dimensional built-up structures with cracks to a fatigue and fracture analysis code that uses stress-intensity factors and material-property data found in "look-up" tables or from equations. NASA is also conducting critical experiments to verify the predictive capabilities of the analysis codes and these tests represent a first step in the technology-validation and

industry-acceptance processes. NASA has established cooperative programs with aircraft manufacturers to facilitate the comprehensive transfer of this technology by making these advanced structural analysis methodologies available to industry. Beta-site testing of the structural analysis codes is well underway and several of these codes have already been integrated into industry's durability and damage-tolerance engineering practices.

# References

(1) Shivakumar, K. N., and J. C. Newman, Jr., "ZIP3D - An Elastic and Elastic-Plastic Finite-Element Analysis Program for Cracked Bodies," NASA TM 102753, 1990.

(2) Potyondy, D. O., "A Software Framework for Simulating Curvilinear Crack Growth in Pressurized Thin Shells", PhD Thesis, Cornell University, Ithica, NY, 1993.

(3) Newman, J. C., Jr., "FASTRAN II - A Fatigue Crack Growth Structural Analysis Program," NASA TM 104159, February 1992.

(4) Wawrzynek, P. A. and A. R. Ingraffea, "FRANC2D: A Two-Dimensional Crack Propagation Simulator Version 2.7 User's Guide," NASA CR 4572, March 1994.

(5) Brogan, F. A., Rankin, C. C., and Cabiness, H. D., "STAGS User Manual," Lockheed Palo Alto Research Laboratory, LMSC Report P032594, 1994.

(6) Potyondy, David. O., Paul A. Wawrzynek, and Anthony R. Ingraffea, "Discrete Crack Growth Analysis Methodology for Through Cracks In Pressurized Fuselage Structures," NASA CP 3274, C. E. Harris, Editor, September 1994, pp. 581-602.

(7) Newman, J. C., Jr., Dawicke, D. S., Sutton, M. A., and C. A. Bigelow, "A Fracture Criterion for Widespread Cracking in Thin-Sheet Aluminum Alloys," Durability and Structural Integrity of Airframes, International Committee on Aeronautical Fatigue, Vol. I, 1993, pp. 443-467.

(8) Forman, R. G., V. Shivakumar, and J. C. Newman, Jr., "Fatigue Crack growth Computer Program "NASA/FLAGRO" Version 2.0," NASA JSC-22276A, May 1994.

(9) Chang, C. C., "A Boundary Element Method for Two Dimensional Linear Elastic Fracture Analysis", PhD Dissertation, The University of Texas, Austin, Texas, December 1993.

(10) Kobayashi, A. S.; Chiu, S. T. and Beeuwkes, R., "A Numerical and Experimental Investigation on the Use of the J-Integral", Engineering Fracture Mechanics, Vol. 5, No. 2, 1973, pp. 293-305.

(11) Andersson, H., "A Finite-Element Representation of Stable Crack Growth," Journal Mechanics and Physics of Solids", Vol. 21, 1973, pp. 337-356.

(12) de Koning, A. U., "A Contribution to Analysis of Slow Stable Crack Growth," National Aerospace Laboratroy MP 75035U, 1975.

(13) Light, M. F.; Luxmoore, A. and Evans, W. T., "Prediction of Slow Crack Growth by a Finite Element Method", International Journal of Fatigue, Vol. 11, 1975, pp. 1045-1046.

(14) Rousselier, G., "A Numerical Approach for Stable-Crack-Growth and Fracture Criteria", Fourth International Conference on Fracture, Waterloo, Canada, Vol. 3, 1977, pp. 1-6.

(15) Shih, C. F.; de Lorenzi, H. G. and Andrews, W. R., "Studies on Crack Initiation and Stable Crack Growth", ASTM STP 668, 1979, pp. 65-120.

(16) Kanninen, M. F.; Rybicki, E. F.; Stonesifer, R. B.; Broek, D.; Rosenfield, A. R. and Nalin, G. T., "Elastic-Plastic Fracture Mechanics for Two-Dimensional Stable Crack Growth and Instability Problems", ASTM STP 668, 1979, pp. 121-150.

(17) Newman, J. C., Jr., "An Elastic-Plastic Finite Element Analysis of Crack Initiation, Stable Crack Growth and Instability", ASTM STP 833, 1984, pp. 93-117.

(18) Brocks, W. and Yuan, H., "Numerical Studies on Stable Crack Growth", ESIS Publicaton 9, 1991, pp. 19-33.

(19) Demofonti, G. and Rizzi, L., "Experimental Evaluation of CTOA in Controlling Unstable Ductile Fracture Propagation", ESIS Publication 9, 1991, pp. 693-70

(20) Paleebut, S., "CTOD and COD Measurements on Compact Specimens of Different Thicknesses," M. S. Thesis, Michigan State, 1978.

(21) Hellman, D. and Schwalbe, K. H., The Crack Tip Opening Displacement in Elastic-Plastic Fracture Mechanic, Springer-Verlag, 1986, pp. 115-132.

(22) Newman, J. C., Jr., Dawicke, D. S., Sutton, M. A. and Bigelow, C. A., "A Fracture Criterion for Widespread Cracking in Thin-Sheet Aluminum Alloys," Proceedings of the ICAF 17th Symposium, 1993.

(23) Broek, D., Thomson, D. and Jeong, D. Y., "Residual Strength of Flat and Curved Fuselage Panels With and Without Widespread Fatigue Damage," U. S. Department of Transportation, Volpe Center, Cambridge, MA, USA, 1993.

# Table 1   NASIP Computer Codes

| Capability \ Codes | FADD* | FRANC2D | ZIP2D | FASTRAN II | STAGS | FRANC3D/STAGS | FRANC3D* | ZIP3D | NASGRO* |
|---|---|---|---|---|---|---|---|---|---|
| Plane Stress/Strain | X | X | X | X | | | | X | |
| Axisymmetry | | X | | | X | | | X | |
| Plate Bending | UD | UD | | | X | X | | | X |
| Thin Shell | | | | | X | X | | | |
| 3D Solid | UD | | | | UD | | X | X | |
| Straight Cracks | X | X | X | X | X | X | X | X | X |
| Curving (nonplaner) Cracks | X | X | | | | X | X | | UD |
| Layered Structure | | UD | | | X | X | | X | |
| Contact | | X | | | X | X | | X | |
| Interface | | X | | | UD | | | | |
| Elasto-Plastic | | UD | X | | X | X | | X | |
| Crack Closure/Variable Amplitude | | | X | X | | | | X | UD |
| Anisotropy | UD | X | | | X | X | | | |
| Residual Strength Analysis | | UD | X | | UD | UD | | X | |
| Graphical Interface | X | X | | | | X | X | | |
| Life Prediction | | | | X | | | | | X |
| Mesh Generation | X | X | | | | X | X | | |
| K vs. A History | X | X | | | X | X | X | | |

*FADD is also implemented into NASGRO and FRANC3D
UD -- under development
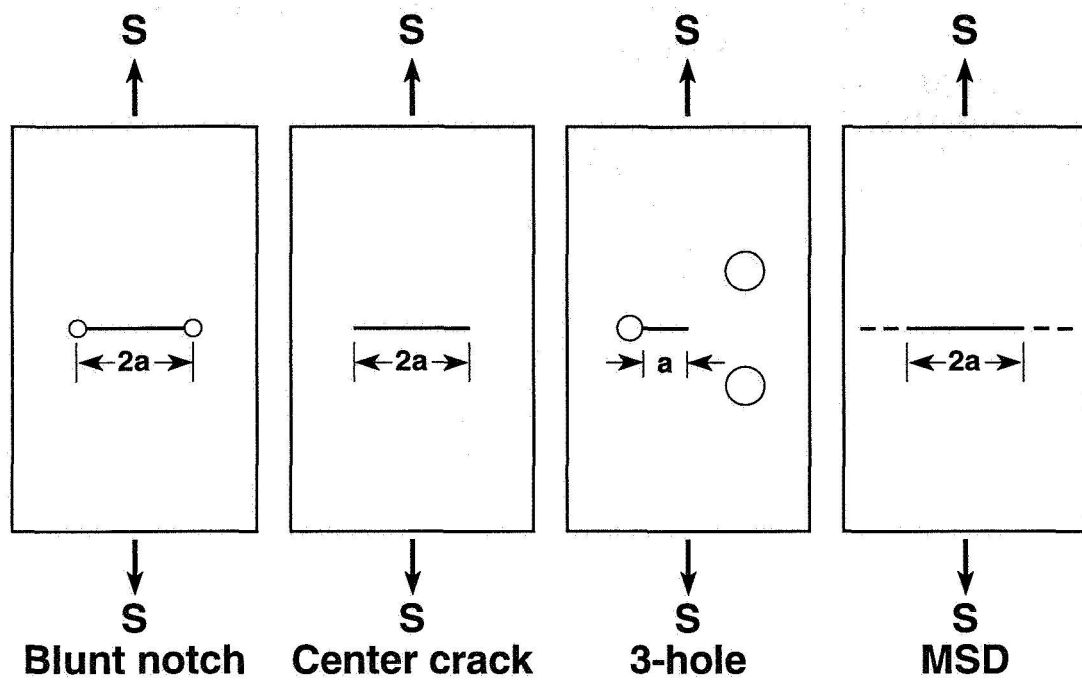
Figure 1.  Fracture specimens for residual strength.
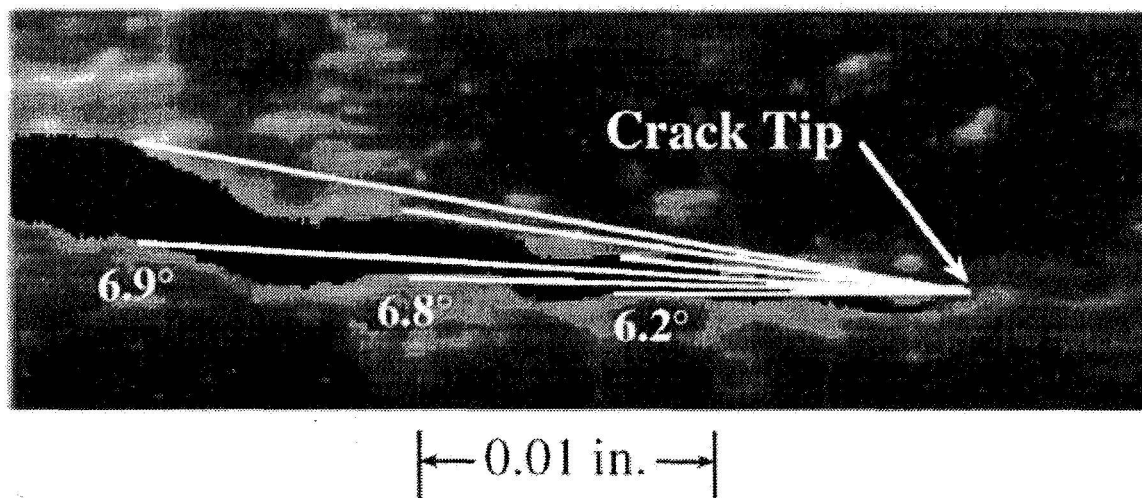


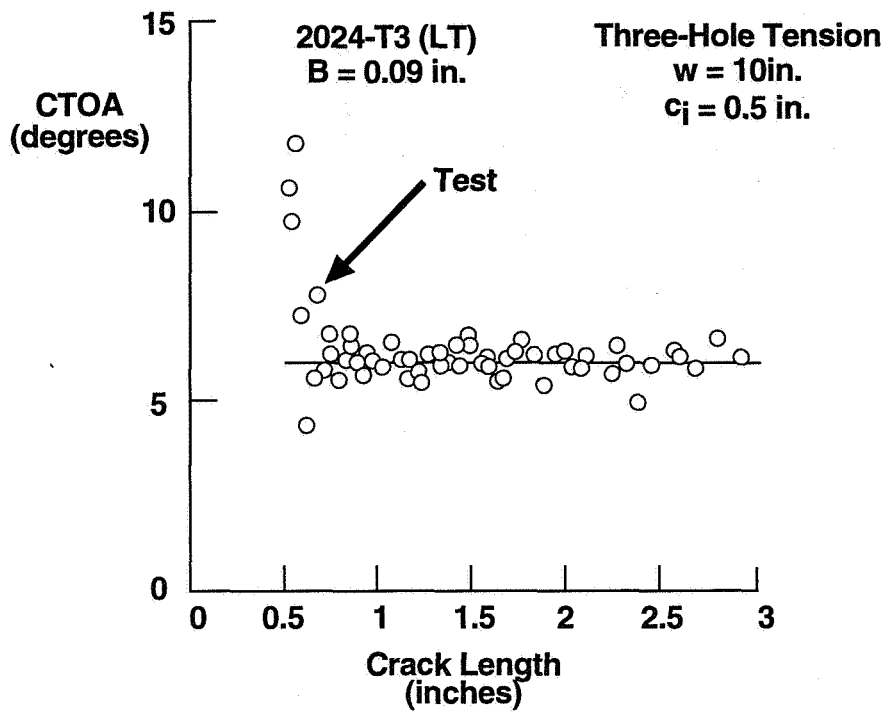Figure 2. Crack-tip opening angle (CTOA) measurements.

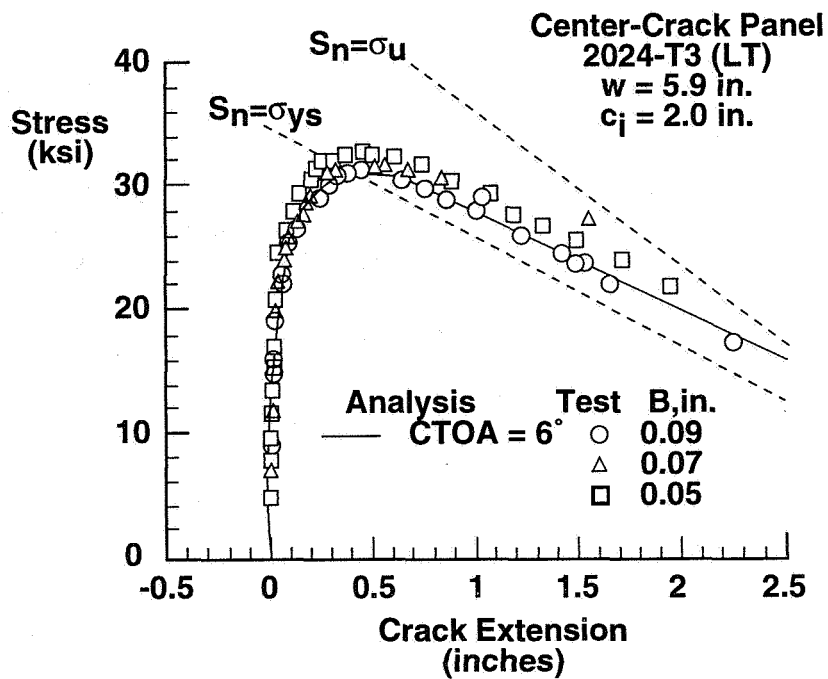Figure 3. Experimental measurements of CTOA.



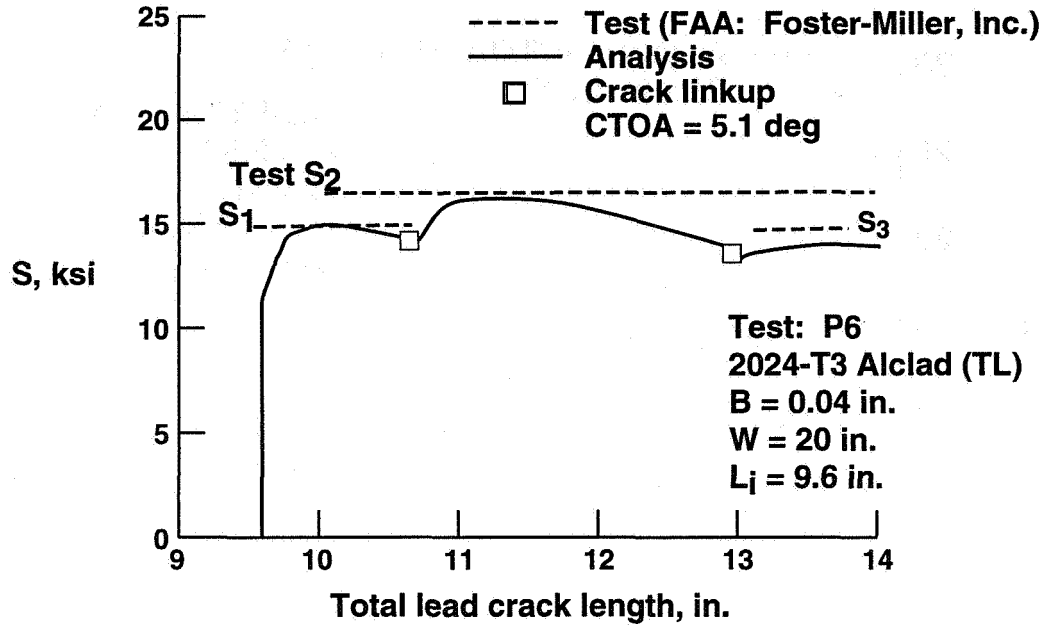Figure 4. Effects of specimen thickness on crack extension.

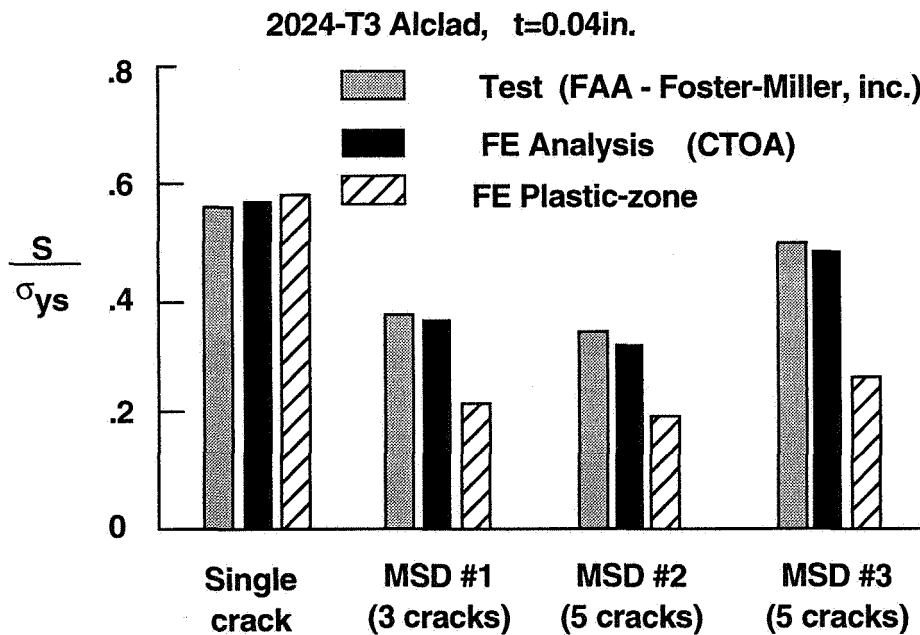Figure 5. Residual strength of panel with long lead crack and 2 MSD cracks.

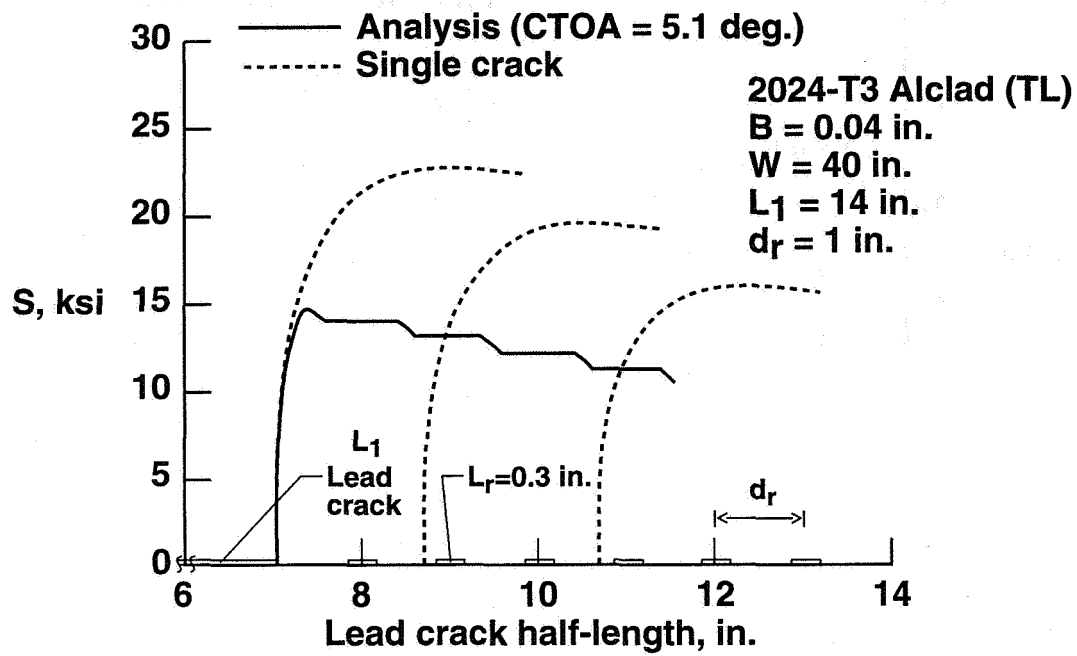Figure 6. Comparison of test and analysis for single crack and MSD configurations.
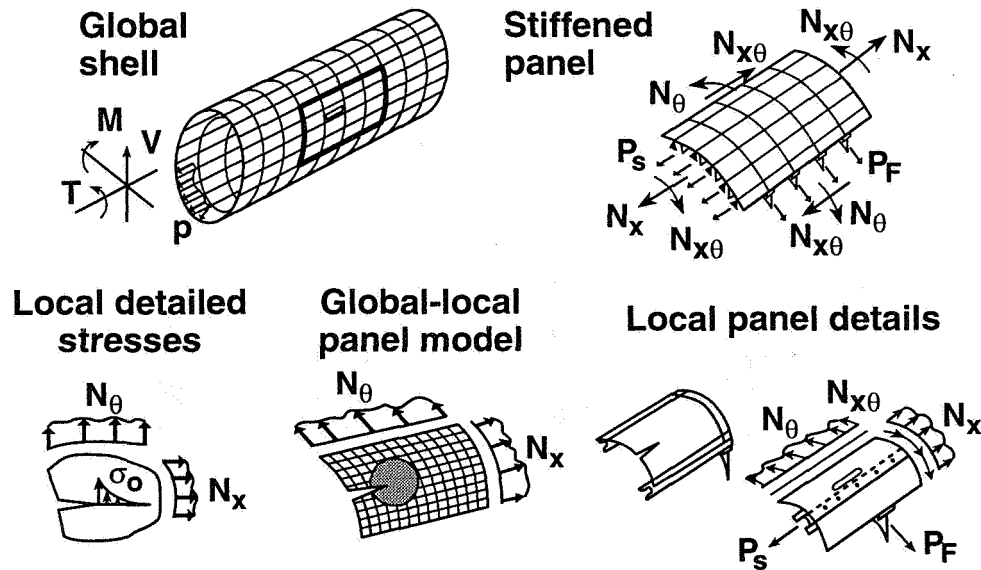
Figure 7. Effect of MSD on residual strength.

Figure 8. Hiearchical nonlinear stiffened shell models.

**Pressure = 8.0 psi**
**Radius = 74 in.**
**Skin thickness = .036 in.**

Max.

**36 Bay Local Model**

Min.

**Resultant Hoop Stress**
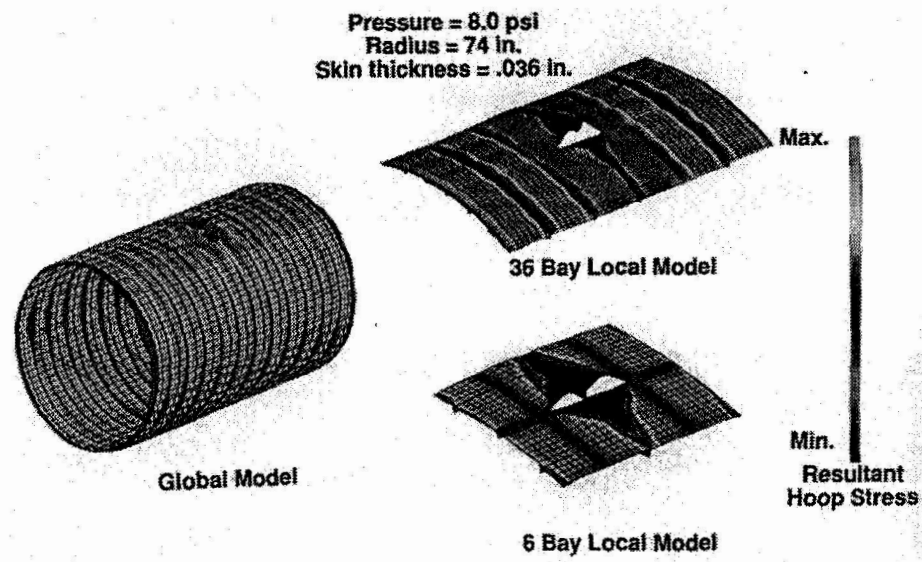
**Global Model**

**6 Bay Local Model**

Figure 9.  Analysis of or results for (also figures 10, 11,12,)
Stiffened aluminum fuselage shell with 20 in.
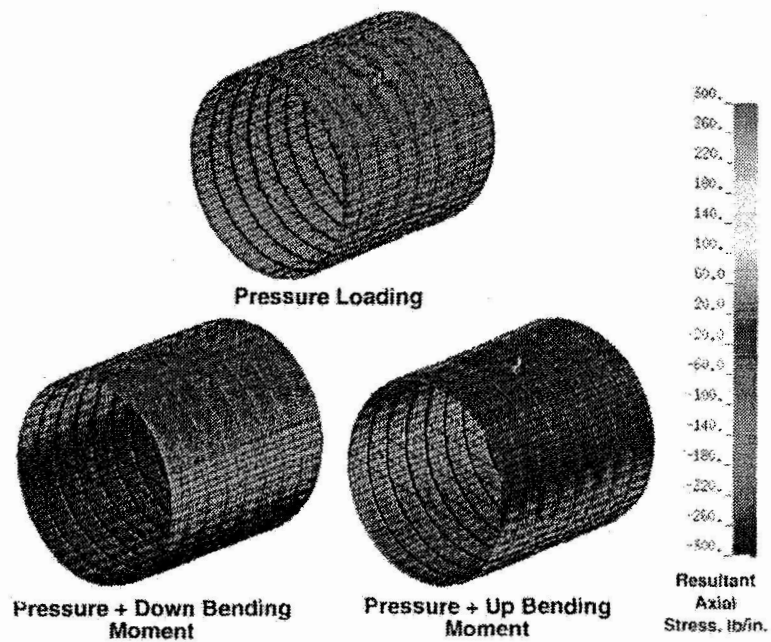longitudinal skin crack and broken frame.



**Pressure Loading**

**Pressure + Down Bending Moment**

**Pressure + Up Bending Moment**

**Resultant Axial Stress, lb/in.**

Figure 10. Global model of stiffened aluminum fuselage
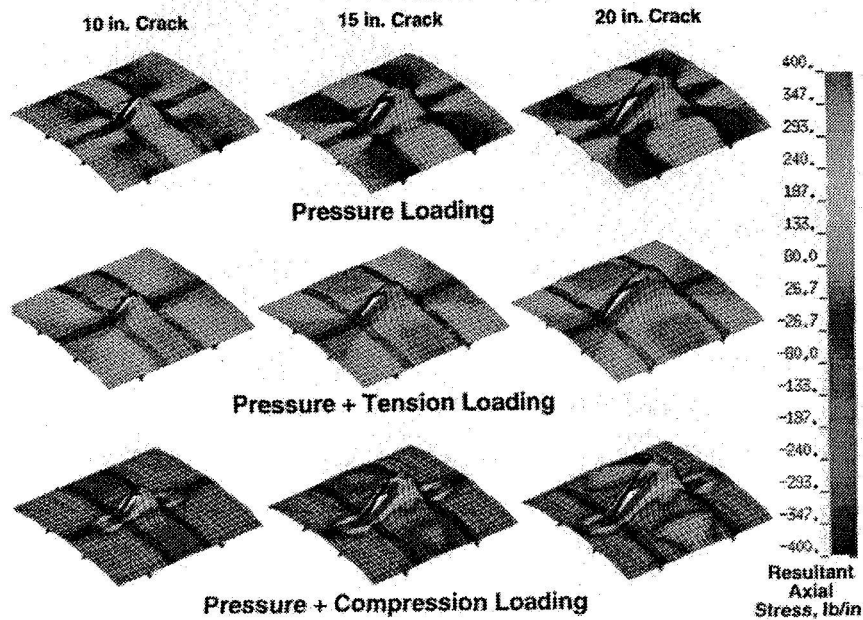shell model with a 10 in. longitudinal skin crack.

23

Figure 11. Two-bay by Three-bay stiffened aluminum fuselage
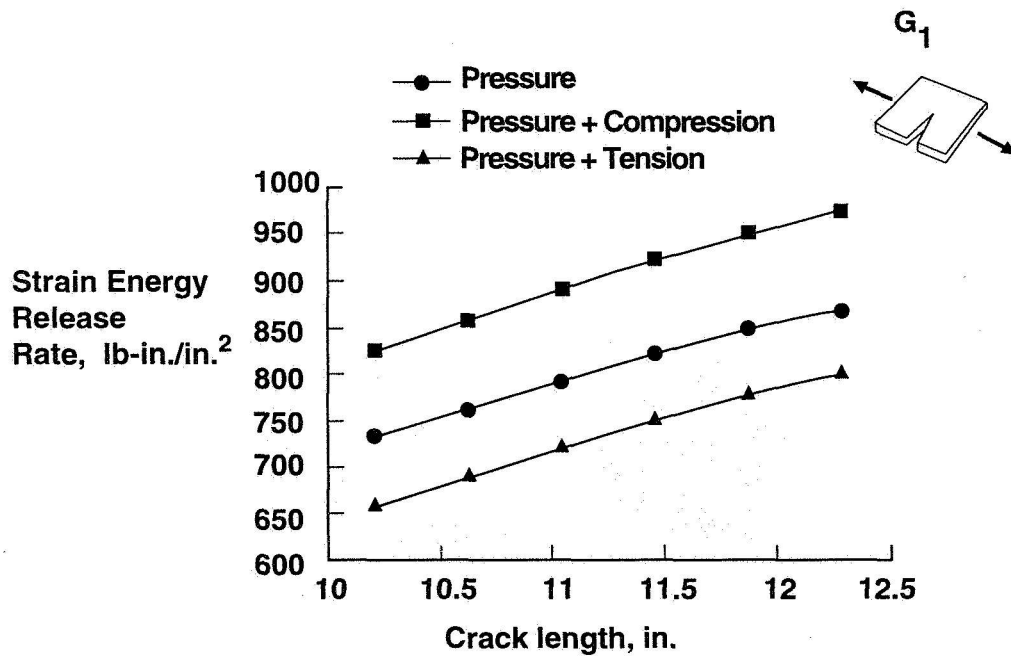shell model with a skin crack.



Figure 12. Two-bay by Three-bay stiffened aluminum fuselage
shell model

# REPORT DOCUMENTATION PAGE

Public reporting burden for this collection of information is estimated to average 1 hour per response, including the time for reviewing instructions, searching existing data sources, gathering and maintaining the data needed, and completing and reviewing the collection of information. Send comments regarding this burden estimate or any other aspect of this collection of information, including suggestions for reducing this burden, to Washington Headquarters Services, Directorate for Information Operations and Reports, 1215 Jefferson Davis Highway, Suite 1204, Arlington, VA 22202-4302, and to the Office of Management and Budget, Paperwork Reduction Project (0704-0188), Washington, DC 20503.

| 1. AGENCY USE ONLY (Leave blank) | 2. REPORT DATE | 3. REPORT TYPE AND DATES COVERED |
|---|---|---|
| | August 1995 | Technical Memorandum |

| 4. TITLE AND SUBTITLE | 5. FUNDING NUMBERS |
|---|---|
| Development of Advanced Structural Analysis Methodologies for Predicting Widespread Fatigue Damage in Aircraft Structures | WU 538-02-10 |

**6. AUTHOR(S)**

Charles E. Harris; James H. Starnes, Jr.; and James C. Newman, Jr.

| 7. PERFORMING ORGANIZATION NAME(S) AND ADDRESS(ES) | 8. PERFORMING ORGANIZATION REPORT NUMBER |
|---|---|
| NASA Langley Research Center<br>Hampton, VA 23681-0001 | |

| 9. SPONSORING / MONITORING AGENCY NAME(S) AND ADDRESS(ES) | 10. SPONSORING / MONITORING AGENCY REPORT NUMBER |
|---|---|
| National Aeronautics and Space Administration<br>Washington, DC 20546-0001 | NASA TM-110187 |

**11. SUPPLEMENTARY NOTES**

Presented at the Sixth International Conference on the Continued Airworthiness of Aircraft Structures, Atlantic City, New Jersey, June 26-29, 1995

| 12a. DISTRIBUTION / AVAILABILITY STATEMENT | 12b. DISTRIBUTION CODE |
|---|---|
| Unclassified - Unlimited<br>Subject Category 39 | |

**13. ABSTRACT (Maximum 200 words)**

NASA is developing a "tool box" that includes a number of advanced structural analysis computer codes which, taken together, represent the comprehensive fracture mechanics capability required to predict the onset of widespread fatigue damage. These structural analysis tools have complementary and specialized capabilities ranging from a finite-element-based stress-analysis code for two- and three-dimensional built-up structures with cracks to a fatigue and fracture analysis code that uses stress-intensity factors and material-property data found in "look-up" tables or from equations. NASA is conducting critical experiments necessary to verify the predictive capabilities of the codes, and these tests represent a first step in the technology-validation and industry-acceptance processes. NASA has established cooperative programs with aircraft manufacturers to facilitate the comprehensive transfer of this technology by making these advanced structural analysis codes available to industry.

| 14. SUBJECT TERMS | | 15. NUMBER OF PAGES |
|---|---|---|
| Durability<br>Damage Tolerance<br>Fracture Mechanics<br>Structural Mechanics | | 25 |
| | | 16. PRICE CODE<br>A03 |

| 17. SECURITY CLASSIFICATION OF REPORT | 18. SECURITY CLASSIFICATION OF THIS PAGE | 19. SECURITY CLASSIFICATION OF ABSTRACT | 20. LIMITATION OF ABSTRACT |
|---|---|---|---|
| Unclassified | Unclassified | | |